Structure of a Transcribing T7 RNA Polymerase Initiation Complex

Graham M. T. Cheetham[1] and Thomas A. Steitz[1,2,3]*

The structure of a T7 RNA polymerase (T7 RNAP) initiation complex captured transcribing a trinucleotide of RNA from a 17–base pair promoter DNA containing a 5-nucleotide single-strand template extension was determined at a resolution of 2.4 angstroms. Binding of the upstream duplex portion of the promoter occurs in the same manner as that in the open promoter complex, but the single-stranded template is repositioned to place the +4 base at the catalytic active site. Thus, synthesis of RNA in the initiation phase leads to accumulation or "scrunching" of the template in the enclosed active site pocket of T7 RNAP. Only three base pairs of heteroduplex are formed before the RNA peels off the template.

In comparison to the multisubunit DNA-dependent RNAPs that synthesize messenger RNA in prokaryotes and eukaryotes (*1, 2*), the DNA-dependent RNAP from a T7 bacteriophage is a relatively simple enzyme (of molecular weight 100 kD) that is capable of transcribing the complete T7 phage DNA. T7 RNAP is homologous to eukaryotic mitochondrial, chloroplast, and other phagelike RNAPs (*3*) and to the well-studied polymerase I (pol I) family of DNA polymerases (*4, 5*). Because it shows most of the functional features that are characteristic of RNAPs, its close relation to the pol I DNA polymerases makes it ideal for understanding the structural bases for the functional differences between DNA and RNA polymerases.

DNA-dependent RNAPs have several functional features not seen in DNA polymerases, although they share a common two-metal-ion mechanism for phosphodiester bond formation (*6*). The RNAPs can initiate transcription, which involves recognition of specific promoter DNA sequences (*7*) followed by melting of the DNA strands close to the catalytic active site and precise positioning of the single-stranded template at positions +1 and +2 for base pairing with incoming ribonucleoside triphosphates. In contrast to DNA polymerases, initiation is primed by a single nucleotide rather than an oligonucleotide. The initiation phase is characterized by abortive cycling, a process of repeated synthesis and release of short RNA products (*8*). During initiation, the template strand and active site must constantly translate in relation to each other while a firm grip of the promoter is retained (*9*). Synthesis of short oligonucleotide products continues until some transition or conformational change occurs to form the more stable elongation complex that is capable of transcribing the complete template. The intermediate DNA-RNA hybrid duplex is analogous to the primer-template DNA homoduplex product synthesized by DNA polymerases. However, in contrast to the DNA polymerase, the transcript peels away from the template and exits the transcribing polymerase complex. A final contrast with the DNA polymerases is that the initiation of transcription by RNAPs is regulated by many protein transcription factors.

The structure of a binary complex formed between T7 RNAP and a 17–base pair open promoter DNA (T7 RPP) (*10*) established that domains present in the RNAP but not in the DNA polymerase are able to recognize specific promoter sequences and denature the duplex to form an initiation bubble. The template base at position −1 is bound in a hydrophobic pocket adjacent to the catalytic active site, and this positions the template strand for initiation by a single nucleotide. On the basis of the structures of this T7 RNAP binary complex, the ternary complex of T7 DNA polymerase (*11*), a model of an initiation complex was constructed with a priming nucleotide at +1 and an incoming nucleoside triphosphate (NTP) at +2.

The structure of a transcribing initiation complex shows that, during synthesis, the template strand has accumulated or scrunched into a pocket in the enzyme to place positions +3 and +4 of the template strand at the catalytic site. Only the 3 base pairs of heteroduplex observed are likely to form before the transcript peels off and exits through its own RNA binding cleft. The specificity for synthesis of RNA rather than DNA transcripts appears to reside largely in the numerous hydrogen bonds made between the protein and 2′-OH of the incoming NTP and each of first three nucleotides of the transcript (at least) as well as the enzyme's structural complementarity to the true A-form heteroduplex. The inhibitory effect on T7 RNAP of T7 lysozyme, which binds to the side of the polymerase opposite the active site (*12*), is achieved, in part, by this transcription factor allosterically altering the structure of the polymerase active site and its suitability for catalysis.

The Structure of a Transcribing RNAP Initiation Complex

Because the cocrystal form of the T7 RNAP initiation complex with promoter DNA, three nucleotides of transcribed RNA, and a ribonucleoside triphosphate analog is nearly isomorphous with the crystal of the binary promoter–T7 RNAP complex (T7 RPP), the new structure could be solved by rebuilding models into difference maps and subsequent coordinate refinement to a crystallographic R factor for 5% of data omitted from refinement, R_{free}, of 0.26% at a resolution of 2.4 Å (*13*). The template extension encodes the RNA transcript 5′-GGGAG at positions +1 though +5. Thus, with the addition of guanosine 5′-triphosphate (GTP) and α,β-methylene adenosine 5′-triphosphate (ATP), the enzyme synthesizes a ribonucleotide trimer, pppGpGpG (p, phosphate group), which can be seen in the experimental difference electron density maps, and then prematurely stalls. The incoming ATP analog and two associated magnesium ions are evident in the 2.8 Å resolution structure of a second isomorphous crystal (*14*). This ATP substrate can be positioned in the first T7 RNAP complex by superposition of 12 C-α atoms located in the active site β strands.

The T7 RNAP in this transcribing quaternary complex (Fig. 1) makes the same interactions with the duplex part of the promoter (−5 to −17) as observed previously in T7 RNAP (*10*), and the protein structures are nearly identical in the two complexes. In contrast, the single-stranded template portion of the open promoter "bubble" (−1 to −4) has a dramatically different conformation. The primer terminus of the RNA transcript (now at +3), the incoming ATP analog, and the template nucleotides to which they are paired have nearly the same location in the active site as was modeled for the incoming and priming NTPs at positions +1 and +2 (*10*) by homology to the T7 DNA polymerase ternary substrate complex (*11*). Thus, as synthesis proceeds down the template, the catalytic and promoter recognition sites maintain the same relative orientation by accumulating or scrunching the transcribed template in a pocket on the enzyme.

Structural studies of DNA polymerases from a variety of organisms (*4, 5, 11, 15–17*) have a common overall shape that has been morphologically compared to a right hand with domains called "thumb," "fingers," and "palm." The active site of T7 RNAP is located in a deep pocket bounded by the polymerase fingers, thumb, and palm subdomains and an NH_2-terminal domain that is unique to the RNAP

[1]Department of Molecular Biophysics and Biochemistry, [2]Department of Chemistry, Yale University, [3]Howard Hughes Medical Institute, New Haven, CT 06520–8114, USA.

*To whom correspondence should be addressed.

(*10*). In contrast, DNA polymerases bind the primer-template DNA homoduplex product in a more open cleft. This difference in the active site has important implications for many of the fundamental differences between DNA-dependent RNAPs and DNA polymerases.

The newly transcribed RNA chain forms a DNA-RNA hybrid duplex inside the pocket (Figs. 1 and 2), has an exact A-form helical conformation, and occupies a position similar to that of the first few base pairs of primer-template DNA duplex product seen in DNA polymerase complexes. The helical axis of the template-RNA heteroduplex is, however, rotated by ~15° toward the thumb subdomain, as compared to the DNA homoduplex product bound to T7 DNA polymerase (*11*). The thumb subdomain of T7 RNAP does not interact with the heteroduplex, as does the primer-template homoduplex in DNA polymerases. The position of the heteroduplex is fixed by a hydrogen bond between the 2′-OH ribose group of G(+2) and the main-chain carbonyl of residue 425. Because of the strict stereochemical requirements for catalysis in the active site, the positions of the ribose rings at the 3′-terminus of the RNA transcript (+3), the 3′-end of the primer strand in DNA polymerase, and the incoming NTPs (+4 in T7 RNAP) are very similar. Thus, the active site of T7 RNAP is able to specifically bind ribonucleotides with C3′-endo ribose puckers and conserve the catalytic geometry in the active site.

The helical axis of the upstream B-form duplex region of the T7 DNA promoter has a similar orientation to that of the heteroduplex, but the two helical axes are offset by ~30 Å (Fig. 1). The promoter duplex is bound to T7 RNAP at a site remote from the active site pocket. Positions −4 through −1 in the template strand connect the DNA-RNA heteroduplex and the DNA homoduplex helices. This single-stranded region is bound within the active site pocket to form part of the upstream transcription bubble. As observed in the T7 RPP structure, the nontemplate strand from positions −3 through −1 is disordered in electron density maps.

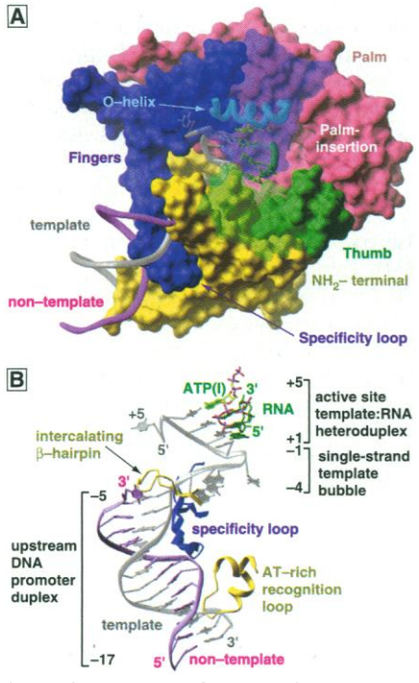

Fig. 1. The structure of a transcribing T7 RNAP complex. (**A**) The position of the template (gray) and nontemplate (purple) DNA, RNA transcript (green), and ATP (light green) on a surface representation of RNAP. The thumb (green) is truncated so the heteroduplex and O helix (light blue) can be seen in the active site pocket. The fingers are blue, the palm is purple, the palm insertion is pink, and the NH_2-terminal domain is yellow. (**B**) The structure of the template strand (gray), nontemplate strand (purple), RNA transcript (green), and next incoming ribonucleoside triphosphate (light green) as seen in the transcribing complex with T7 RNAP. The template-RNA heteroduplex is an A-form helix that is displaced from the upstream promoter duplex. Polymerase elements interacting with the promoter duplex are shown. Figures 1, 2, 3, and 5 were generated with the program RIBBONS (*39*).

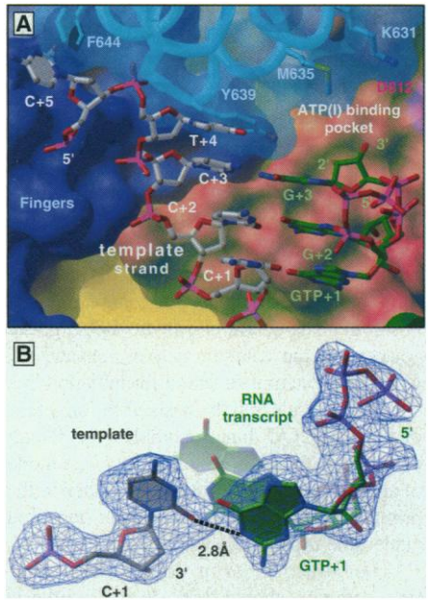

Fig. 2. The active site heteroduplex. (**A**) The pppGpGpG RNA transcript (green) and DNA template (gray) on a surface rendition of the active site pocket and color coded as in Fig. 1 (*40*). Residue Y639 from the end of the O helix interacts with T+4 and partly overlaps the ATP(I) binding site in the complex missing the ATP. Residues M635 and T636 are conserved in phagelike RNAPs and provide the hydrophobic surface against which the base of NTP(I) packs. (**B**) Peeling of the transcript away from the template after four base pairs. Electron density for the mismatched base pair at position +1 is shown. Dashed line indicates single hydrogen bond.

Specificity of T7 RNAP for Synthesizing RNA Rather Than DNA

There are several important ways in which this pol I family RNAP differs from the homologous T7 DNA polymerase; these differences enable it to synthesize RNA rather than DNA transcripts. Not only does this enzyme selectively bind and incorporate ribonucleotides rather than deoxyribonucleotides, but it also binds the 2′-OH groups of the transcript RNA and accommodates the C3′-endo ribose conformation. DNA polymerases enforce specificity for the incorporation of deoxyribose nucleotides because a bulky residue ("steric gate") sterically excludes ribose (*19*). In T7 DNA polymerase, the residue Glu^{480} functions as a steric gate. The corresponding residue in T7 RNAP is Gly^{542}, which is absolutely conserved in phagelike RNAPs. The lack of any side chain allows the 2′-OH of the incoming ribonucleoside triphosphate to be accommodated. Residue His^{784} can move toward and directly interact with the 2′-OH ribose position of NTP(I). In DNA polymerase, the position corresponding to His^{784} is usually occupied by glutamine (Fig. 3), which is constrained to adopt an alternate side-chain rotamer because of the steric gate residue, Glu^{480}. Residue Tyr^{639} is also within hydrogen-bonding distance of the 2′-OH of NTP(I), although it is disordered in the quaternary complex.

The "O helix" in the fingers subdomain of pol I family polymerases contains a highly conserved sequence motif that is important for binding the incoming nucleotide. However, its conformation in T7 RNAP is different from that in the homologous DNA polymerases. Residue Tyr^{639}, homologous to Tyr^{766} in *Escherichia coli* DNA polymerase I, Tyr^{530} in T7 DNA polymerase, and Tyr^{714} in *Bacillus* DNA polymerase (*19*), is located in a loop region immediately adjacent to the O helix. It is not part of the helix, as observed in DNA polymerase, but adopts a novel position with respect to NTP(I). The mutation $Tyr^{639} \rightarrow Phe^{639}$ substantially reduces the preference of T7 RNAP for ribonucleotide over deoxyribonucleotide substrates (*20*). It also increases the misincorporation of bases and the extension of short RNA transcripts. An analogous mutation, $Tyr^{766} \rightarrow Phe^{766}$, in *E. coli* DNA polymerase I affects the fidelity of deoxyribonucleotide incorporation (*21*). These data suggest that residue Tyr^{639} may have a multifunctional role in RNAP, which may be different than its role in DNA polymerase. Additional mutations suggest that Tyr^{639} may distinguish between GTP(I) and ATP(I) (*22*).

The phenolic ring of Tyr^{639} plays a role in positioning the +3 ribonucleotide and, consequently, NTP(I) (Fig. 2A) by stacking against the template base (+3), which is paired with the primer terminus. It also helps to redirect the template strand away from the active site across the face of the fingers subdomain so that posi-

tion +5 stacks against residue Phe^{644}, in a similar manner to that seen in human immunodeficiency virus (HIV)–type 1 reverse transcriptase (*23*). On the basis of the observed position of the incoming nucleoside, ATP(I), and the position of the +4 template base in this structure, the phenolic ring of residue Tyr^{639} partially overlaps with the ATP(I) binding pocket when the ATP(I) is not present. It appears that residue Tyr^{639} can compete with NTP(I) for similar positions within the T7 RNAP active site. The role of residue Tyr^{639} in T7 RNAP, seen in our structure, is therefore very similar to that of residue Tyr^{714} in the structures of *Bacillus* DNA polymerase complexed with several DNA substrates (*19*).

There are other important structural differences between T7 RNAP and the homologous DNA polymerases that enable it to specify the formation of an RNA-DNA heteroduplex. Discrimination between ribose and deoxyribose is achieved, in part, by hydrogen bonding between the protein and the 2′-OH groups of the growing RNA transcript. Specificity for the 2′-OH at the primer terminus, NTP(P), is achieved by a direct hydrogen bond between Arg^{425} and the 2′-OH ribose group. Residue Arg^{425} also hydrogen bonds to the N3 position of G+3 (and could make similar contacts with the N3 position of A or with the O2 position of U and C), located in the minor groove of the A-form template-RNA hybrid. In the T7 DNA polymerase (*11*) and the *Thermus aquaticus* DNA polymerase (*17*), primer-template complexes (residues Arg^{429} and Arg^{573}, respectively) make only a single hydrogen bond with the O4′ deoxyribose position of the primer 3′-terminus. The constraints imposed on the position and orientation of residue Arg^{425} by the surrounding side chains in T7 RNAP therefore define a unique binding site for ribonucleotides with C3′-endo ribose conformation. The 2′-OH of the second nucleotide from the primer terminus, G(+2), is hydrogen bonded to a backbone carbonyl oxygen.

The binding site for the RNA-DNA heteroduplex is complementary to the true A-form duplex rather than to the conformation seen with DNA polymerases (*11, 17, 19, 24*). The ribose backbone of the heteroduplex bound to T7 RNAP superimposes on the crystal structure of an RNA-DNA heteroduplex (*25*) with a root mean square deviation (rmsd) of 1.0 Å and on the corresponding portion of the primer template bound to T7 DNAP with a rmsd of 1.9 Å. Unlike duplex DNA bound to DNA polymerases, the heteroduplex shows all the characteristics of A form, including base pairs being tilted and displaced in relation to the helix axis.

Substrate-Induced Conformational Changes in T7 RNAP

The three DNA polymerases and HIV reverse transcriptase structural studies have shown a substantial rotation of the fingers domain upon binding of dNTP to the polymerase-DNA binary complex (*26*). This large rotation in the fingers subdomain orients catalytically important amino acids located in the O helix (which is conserved in the pol I family) or in an analogous feature in other polymerase families. In the transcribing complexes of T7 RNAP, reported here, the fingers subdomain is considerably more closed than in either the unliganded (*27*) or T7 lysozyme complex (*12*) crystal structures. However, the arrangement of polymerase domains are unchanged with respect to the binary T7 RPP complex. Although this closing of the polymerase conformation upon promoter binding by T7 RNAP is small (in relation to the differences observed in the DNA polymerases), it is sufficient to move residue Lys^{631}, which interacts with the triphosphate moiety of the incoming ribonucleotide substrate (*28*), and residue Tyr^{639} 6 Å closer to the catalytic active site.

Regulation of T7 RNAP Activity by T7 Lysozyme

T7 lysozyme appears to inhibit transcription by T7 RNAP in part by allosterically changing the T7 RNAP active site structure. In the complex between T7 RNAP and T7 lysozyme (*12*), the COOH-terminal residues and the closely associated active site of T7 RNAP are in an altered conformation when compared to the transcribing complex described here.

The catalytic active site of T7 RNAP is located on the surface of three β strands in the palm subdomain, which lies between the fingers and thumb subdomains. The COOH-terminal residues of T7 RNAP and other phage-like RNAPs have a sequence that is highly conserved and occupy a position that is similar to that occupied by a fourth β strand seen in homologous DNA polymerase structures. In the absence of a bound promoter, residues Phe^{882}-Ala^{883}-COOH can be cleaved in solution by carboxypeptidase A; however, this "FOOT" becomes resistant to proteolysis during transcription initiation (*29*). In the T7 RNAP–T7 lysozyme complex (*12*), the partially ordered FOOT adopts an extended conformation, whereas in the transcribing complex, Phe^{882} and Ala^{883} are bound in a hydrophobic pocket beneath the three β strands. This protects them from proteolysis and induces a structural rearrangement in the active site conformation that orients the catalytically essential residues, Asp^{537} and Asp^{812} (*28*) (Fig. 4), and thus creates the binding sites for magnesium ions and ribonucleotide substrates.

Thus, it appears that the T7 lysozyme interaction with T7 RNAP inhibits the binding of the COOH-terminal FOOT to the palm subdomain, thereby inhibiting the formation of an active site that can stably bind NTP and RNA transcript in the initial stages of transcription. This is consistent with an observed reduced affinity of the T7 RNAP–lysozyme complex for NTPs (*30*). The palm-insertion module (residues 450 through 527) (*27*), which is not present in DNA polymerase, closes in behind the FOOT, preventing it from retracting out of its hydrophobic binding site. The FOOT is located beneath the active site, more than 8 Å away from the catalytically essential carboxylate residues, and is not in a position to interact with either the incoming ribonucleotide substrate or RNA transcript, as had previously been suggested (*31, 32*).

Length of the Transcript-Template Heteroduplex

It appears that the intermediate heteroduplex cannot extend beyond a total of four base pairs, including the interaction of the template with the next incoming substrate, NTP(I). Extension of the template-RNA heteroduplex in the active site pocket by even one additional base pair would result in clashes with the polymerase NH_2-terminal domain. The non–Watson-Crick

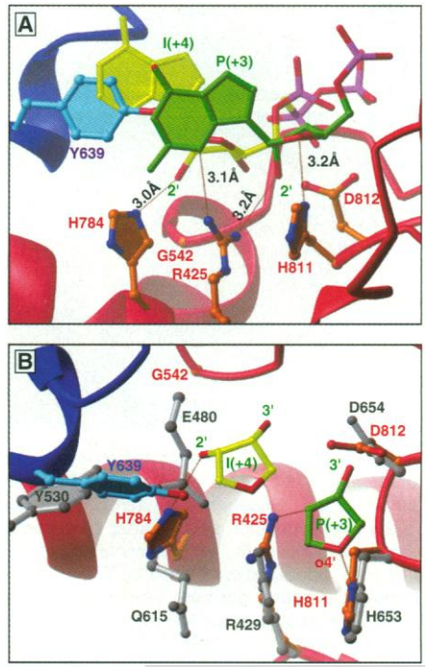

Fig. 3. Comparison of the nucleotide binding sites in T7 RNAP (red and blue) and T7 DNA polymerase (gray). The structures were aligned by superimposing 15 C-α positions located in three corresponding active site β strands. The secondary structure of only T7 RNAP is depicted as ribbons, whereas T7 DNA polymerase residues are gray (*40*). Side chains in palm and fingers subdomains are red and blue, respectively. (**A**) The structures of ATP(I+4) (light green) and primer terminus (P+3) (green) at the active site with selected important interactions with T7 RNAP interactions. (**B**) Comparison with T7 DNAP viewed from the top of (A). Residues Y639 and Y530 are in dramatically different orientations, whereas H784 and R425 interact with 2′-OH groups. The ribose groups for the +3(P) and +4(I) substrates in T7 RNAP are shown in green.

base pair seen at position +1, 3 base pairs from the primer terminus, is likely to end the heteroduplex (Fig. 2). The single hydrogen bond between the template base C(+1) and pppG base at the 5′-end of the RNA product may be the point at which the transcript starts to peel away from the template (Fig. 2B). In contrast, the open cleft in DNA polymerases allows the primer-template DNA homoduplex product to extend out of the enzyme as a continuous duplex.

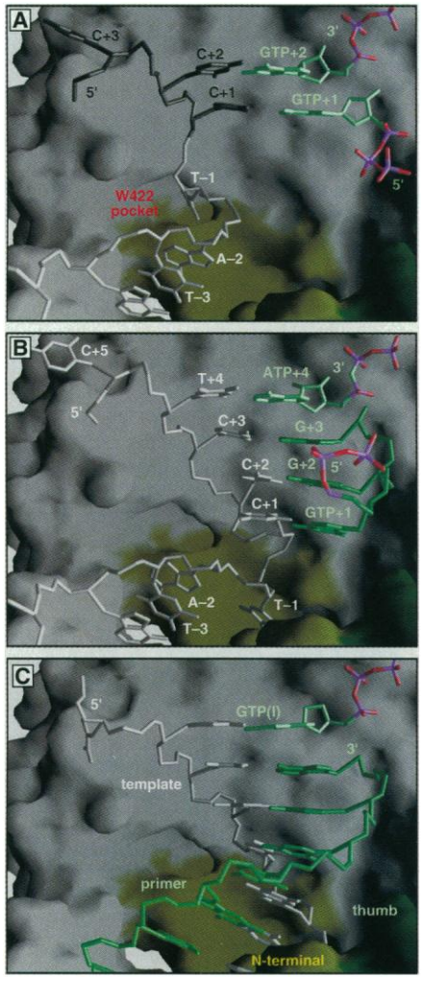

Fig. 4. Experimental evidence for scrunching of the template in the active site pocket. The structures of the single-stranded template strand (gray) (**A**) at initiation and (**B**) after synthesis of three nucleotides. (A) Before formation of the first 3′-5′ phosphodiester bond by T7 RNAP, the template strand at position–1 binds in a hydrophobic pocket adjacent to the catalytic active site (1; white) (*40*). This orients the +1 and +2 template positions (dark gray) to create the binding sites for two GTP substrates (light green) in the incoming and priming positions. The template strand overhang (positions +1 through +3) and the GTP substrates were modeled on the basis of the T7 DNA polymerase structure and the transcribing T7 RNAP complex. (B) After synthesis of pppGpGpG (dark green), the +3 and +4 positions of the template strand are now located in priming and incoming positions. The template base T–1 flips out of the small hydrophobic pocket into the larger active site pocket. The structure of template residues T–3 to T–1 has completely changed. (**C**) Extension of a primer template beyond three base pairs taken from the T7 DNA polymerase structure results in clashes with the protein. Figure 4 was generated with the program GRASP (*41*). Thumb subdomain and NH_2-terminal domain are green and yellow, respectively.

DNA Scrunching During Transcription Initiation and Abortive Cycling

Ikeda and Richardson (*9*) have previously shown that, upon synthesis of pppGpGpG, the footprint of T7 RNAP on the template strand is extended in the downstream direction from position +3 to position +8. In contrast, the upstream footprint remains constant, consistent with the enzyme-retaining interactions with the upstream promoter duplex during initiation and abortive cycling. Only after the synthesis of an 8- to 10-nucleotide (nt) RNA transcript (*32*) and transition to processive RNA synthesis does T7 RNAP release the upstream promoter contacts. Thus, during abortive cycling, the downstream contacts between the polymerase and the template expand and contract while the upstream contacts are constant. These footprinting data are consistent with three popular models for transcription initiation: "polymerase inchworming," in which the enzyme progressively extends on the downstream template and nontemplate strands; "DNA scrunching," in which the conformation of the polymerase remains unchanged while the transcribed template strand accumulates within the active site pocket; and a third model in which the DNA slides forward and back.

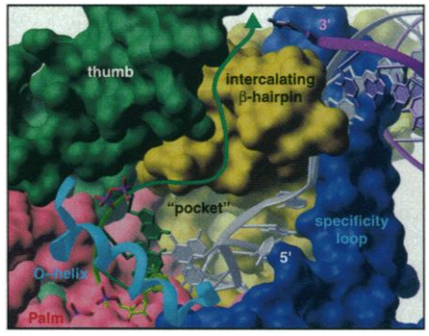

Fig. 5. The active site pocket and transcript exit channel. A view of the active site with the protein represented as a surface. The polymerase thumb subdomain (green), NH_2-terminal domain (yellow), specificity loop (blue), and palm (purple) from the active site pocket. The deep pocket into which the single-stranded template (gray) accumulates is highly positively charged and adjacent to the exit channel for the RNA transcript. The remaining volume of the active site pocket is sufficient to accommodate a further four-template-strand base (eight in total), enabling the RNA transcript (8-nt oligomer) to bridge the gap to the exit channel. A possible binding site for the transcript exiting the active site is shown by a green arrow. The fingers subdomain has been removed to reveal the pocket.

Comparison of the crystal structure of the transcribing RNAP with that of the T7 RPP complex (*10*) provides the first direct structural evidence for accumulation or scrunching of nucleic acid chains in the catalytic active site. In order to position the template base at +4 in the active site opposite the incoming NTP(I), the single-stranded template substantially changes its conformation within the active site pocket (Fig. 5). The template base at position −1 orients the +1 and +2 template positions to bind two guanosine ribonucleotide triphosphate substrates during the first step of initiation. After the synthesis and translocation of a trinucleotide, the base at −1 has flipped out of the hydrophobic pocket formed by Trp^{422}, His^{300}, and Tyr^{739} and has assumed a new position (Fig. 4). In contrast, the structure of the protein does not change substantially during this process. The polymerase and NH_2-terminal domains of these two complexes superimpose with a rmsd of 0.84 Å for all 862 C-α positions. Thus, it appears that the template is accumulating in the active site as RNA synthesis proceeds.

The volume of the active site pocket appears to be sufficient to accommodate the template required to synthesize a transcript that is 6 to 9 nt long. Its volume is defined by the positions of the base pair at +1 and the NH_2-terminal domain and is ~3850 $Å^3$ (Fig. 5). This volume is sufficient to accommodate four further template bases (eight template bases in total) in the active site pocket, assuming an approximate solvent content of 30% and a Matthews coefficient, V_m (*33*), equal to 1.9 to 2.0. Thus, the observed average transcript length of abortive products (8 to 10 bases) (*32*) and the number of template bases that can be accommodated appear to be correlated.

Escape from the Initiation Phase to Processive Elongation

We hypothesize that the escape from abortive cycling to the processive elongation phase occurs when the additional template can no longer be accommodated in the active site pocket and the transcript is long enough to bind tightly to the NH_2-terminal domain. Once the electrostatically positive pocket is filled with the template, either the message dissociates and synthesis begins again (abortive synthesis) or the duplex promoter releases from the protein to allow removal of the template. A longer transcript is likely to favor the latter possibility, because a transcript-induced change in the thumb conformation might allow it to cover the cleft, thereby forming a tunnel through which the elongating RNA would pass.

References and Notes

1. R. Tjian, *Philos. Trans. R. Soc. London Ser. B* **351**, 491 (1996).
2. R. L. Tracy and D. B. Stern, *Curr. Genet.* **28**, 205 (1995).

3. B. Hedtke, T. Börner, A. Weihe, *Science* **277**, 809 (1997).
4. D. L. Ollis, P. Brick, R. Hamlin, N. G. Xuong, T. A. Steitz, *Nature* **313**, 762 (1985).
5. C. A. Brautigam and T. A. Steitz, *Curr. Opin. Struct. Biol.* **8**, 54 (1998).
6. T. A. Steitz, S. J. Smerdon, J. Jäger, C. M. Joyce, *Science* **266**, 2022 (1994).
7. P. H. von-Hippel, D. G. Bear, W. D. Morgan, J. A. McSwiggen, *Annu. Rev. Biochem.* **53**, 389 (1984).
8. A. J. Carpousis and J. D. Gralla, *Biochemistry* **19**, 3245 (1980).
9. R. A. Ikeda and C. C. Richardson, *Proc. Natl. Acad. Sci. U.S.A.* **83**, 3614 (1986).
10. G. M. T. Cheetham, D. Jeruzalmi, T. A. Steitz, *Nature* **399**, 80 (1999).
11. S. Doublié, S. Tabor, A. M. Long, C. C. Richardson, T. Ellenberger, *Nature* **391**, 251 (1998).
12. D. Jeruzalmi and T. A. Steitz, *EMBO J.* **17**, 4101 (1998).
13. Crystals of the quaternary complex reported here were grown similarly to those of the binary complex described previously (*10*); T7 RNAP was mixed (0.3 mM) with a T7 promoter (0.35 mM), in the presence of ribonucleotides GTP, uridine 5′-triphosphate, cytidine 5′-triphosphate, and α,β-methylene ATP (4 mM each) and 15 mM $MgCl_2$. The promoter was constructed by annealing together two synthetic oligonucleotides that consisted of a 22-nt template strand of sequence 5′-CTCCCTATAGTGAGTCGTATTA-3′ and a 17-nt nontemplate strand of sequence 5′-TAATACGACTCACTATA-3′. This produced a 17–base pair duplex and a 5-nt template overhang. In this way, the T7 RNAP synthesized a 3-nt RNA and stopped at position +4 of the template strand before crystallization. Data were collected at Brookhaven National Laboratory (station X25), using x-rays of wavelength 1.10 Å, which were recorded with a Brandeis B4 charge-coupled device detector and reduced with the program MOSFLM (*34*). The crystals are orthorhombic space group $P2_12_12$ with cell dimensions of a = 221.2 Å, b = 73.6 Å, and c = 80.9 Å. The number of unique reflections recorded was 51,537 (97.8% complete, with 40 to 2.4 Å resolution), with an overall multiplicity of 3.8 and a crystallographic R factor for merging all data (40 to 2.4 Å), R_{merge}, of 0.078. Subsequent analysis was performed with the CCP4 software suite (*35*). Despite an R factor of 24% between these data and data from the T7 RPP complex, the template strand 5′-overhang and 5′-pppGpGpG-3′ RNA transcript could clearly be seen in difference Fourier maps calculated with the observed amplitudes from the two crystals and phases derived from the T7 RPP coordinates. The initial crystallographic R factor for the completed model was 0.40 (R_{free} = 0.42). Model refinement (*36*) and rebuilding (*37*) reduced the R factor to 0.22 (R_{free} = 0.26) for all data at a 40 to 2.4 Å resolution; $F > 2\sigma(F)$.
14. The absence of α,β-methylene ATP in these crystals may have resulted from its loss by diffusion when the crystals were soaked in cryoprotection solution: The Michaelis constant K_m for the interaction between T7 RNAP and the NTP in the incoming binding site is ~0.1 mM, determined for optimized in vitro transcription conditions (*38*), and α,β-methylene ATP has poor solubility at high concentrations of polyethyleneglycol/propyleneglycol solution. Alternatively, however, the conformation of the enzyme in this crystal form may play an important role in determining the captured transcription intermediate. Several other crystals that diffracted to a resolution of 2.8 Å clearly have bound magnesium ions and partially occupied α,β-methylene ATP at the +4 position in the active site. In this instance, the template strand and residue Tyr^{639} appear to be poorly ordered in electron density maps.
15. L. A. Kohlstaedt, J. Wang, J. M. Friedman, P. A. Rice, T. A Steitz, *Science* **256**, 1783 (1992).
16. J. Wang *et al.*, *Cell* **89**, 1087 (1997).
17. Y. Li, S. Korolev, G. Waksman, *EMBO J.* **17**, 7514 (1998).
18. G. Gao, M. Orlova, M. M. Georgiadis, W. A. Hendrickson, S. P. Goff, *Proc. Natl. Acad. Sci. U.S.A.* **94**, 407 (1997).
19. J. R. Kiefer, C. Mao, J. C. Braman, L. S. Beese, *Nature* **391**, 304 (1998).
20. R. Sousa and R. Padilla, *EMBO J.* **14**, 4609 (1995).
21. M. Astatke, N. D. F. Grindley, C. M. Joyce, *J. Biol. Chem.* **270**, 1945 (1995).
22. V. O. Rechinsky, D. A Kostyuk, V. L. Tunitskaya, S. N. Kochetkov, *FEBS Lett.* **306**, 129 (1992).
23. H. Huang, R. Chopra, G. L. Verdine, S. C. Harrison, *Science* **282**, 1669 (1998).
24. S. H. Eom, J. Wang, T. A. Steitz, *Nature* **382**, 278 (1996).
25. A. H. Wang *et al.*, *Nature* **299**, 601 (1982).
26. T. A. Steitz, *J. Biol. Chem.* **274**, 17395 (1999).
27. R. Sousa, Y. J. Chung, J. P. Rose, B.-C. Wang, *Nature* **364**, 595 (1993).
28. P. A. Osumi-Davis, M. C. Aguilera, R. W. Woody, A. Y. M. Woody, *J. Mol. Biol.* **226**, 37 (1992).
29. L. P. Gardner, K. A. Mookhtiar, J. E. Coleman, *Biochemistry* **36**, 2908 (1997).
30. J. Villemain and R. Sousa, *J. Mol. Biol.* **281**, 793 (1998).
31. J. Lykke-Andersen and J. Christiansen, *Nucleic Acids Res.* **26**, 5630 (1998).
32. C. T. Martin, D. K. Muller, J. E. Coleman, *Biochemistry* **27**, 3966 (1988).
33. B. M. Matthews, *J. Mol. Biol.* **33**, 491 (1968).
34. A. G. W. Leslie, *Joint CCP4 and ESF-EACMB Newsletter Protein Crystallography No. 26* (Daresbury Laboratory, Warrington, UK, 1992).
35. Collaborative Computational Project No. 4, *Acta Crystallogr.* **D50**, 760 (1994).
36. A. T. Brünger et al., *Acta Crystallogr.* **D54**, 905 (1998).
37. T. A Jones, J. Y. Zou, S. W. Cowan, M. Kjeldgaard, *Acta Crystallogr.* **A47**, 110 (1991).
38. J. L. Oakley, R. E. Strothkamp, A. H. Sarris, J. E. Coleman, *Biochemistry* **18**, 528 (1979).
39. M. Carson, *J. Appl. Crystallogr.* **24**, 958 (1991).
40. Single-letter abbreviations for the amino acid residues are as follows: D, Asp; E, Glu; F, Phe; G, Gly; H, His; K, Lys; M, Met; Q, Gln; R, Arg; W, Trp; and Y, Tyr.
41. A. Nicholls, R. Bharadwaj, B. Honig, *Biophys. J.* **64**, A166 (1993).

42. We thank J. Ippolito, D. Kennedy, and J. Wang for discussions and P. Eatherton for assistance in the preparation of this manuscript. This research was supported by NIH grant number GM-22778 (T.A.S.). The complete refined coordinates of the T7 RNAP transcribing complex and the observed structure factor amplitudes have been deposited in the Protein Data Bank with numbers 1QLN and R1QLNSF.

5 October 1999; accepted 15 November 1999

REPORTS

Phase-Coherent Amplification of Matter Waves

Mikio Kozuma,[1] Yoichi Suzuki,[1] Yoshio Torii,[2] Toshiaki Sugiura,[1] Takahiro Kuga,[1] E. W. Hagley,[3] L. Deng[3]

Phase-coherent matter-wave amplification was demonstrated using Bose-Einstein–condensed rubidium-87 atoms. A small seed matter wave was created with coherent optical Bragg diffraction. Amplification of this seed matter wave was achieved by using the initial condensate as a gain medium through the superradiance effect. The coherence properties of the amplified matter wave, studied with a matter-wave interferometer, were shown to be locked to those of the initial seed wave. The active matter-wave device demonstrated here has great potential in the fields of atom optics, atom lithography, and precision measurements.

Advances in laser science and technology have been supported by the development of a variety of optical elements that can be categorized as either passive or active. Mirrors, beam splitters, and polarizers are typical examples of passive elements, whereas devices such as optical pulsed-dye amplifiers (*1*) are active ones. By passing through such an active device, a weak laser beam can be amplified while maintaining its phase coherence: the mechanism of lasing itself.

In the field of atom optics it has long been speculated, in direct analogy with optical amplifiers, that it should be possible to coherently amplify a matter wave by using an appropriate gain medium. Bose-Einstein condensation (the macroscopic occupation of a single quantum state) in dilute alkali gases (*2, 3*) has the potential of being such a gain medium because it is an ideal source of highly coherent matter waves. What has long since happened for the optical laser is now becoming a reality for matter waves. In fact, many passive matter-wave elements have already been demonstrated. For example, Bragg diffraction (*4*) of a Bose-Einstein condensate (BEC) by a moving, optical standing wave (*5*) can be used to coherently diffract any fraction of a BEC into a selectable momentum state, making it an ideal mirror or beam splitter. These passive elements were key in the development of a highly efficient (nearly 100% contrast) Mach-Zehnder BEC interferometer (*6, 7*). In addition, most

[1]Institute of Physics, University of Tokyo, 3-8-1 Komaba, Meguro-ku, Tokyo 153-8902, Japan. [2]Department of Physics, Gakushuin University, Mejiro 1-5-1, Toshima-ku, Tokyo 171-8588, Japan. [3]Physics Lab, National Institute of Standards and Technology, Gaithersburg, MD 20899, USA.

References and Notes

[1] **The Biochemistry of Transcription in Eukaryotes: A Paradigm for Multisubunit Regulatory Complexes**
Robert Tjian
Philosophical Transactions: Biological Sciences, Vol. 351, No. 1339, Transcription Factors. (Apr. 29, 1996), pp. 491-499.
Stable URL:
http://links.jstor.org/sici?sici=0962-8436%2819960429%29351%3A1339%3C491%3ATBOTIE%3E2.0.CO%3B2-O

[3] **Mitochondrial and Chloroplast Phage-Type RNA Polymerases in Arabidopsis**
Boris Hedtke; Thomas Börner; Andreas Weihe
Science, New Series, Vol. 277, No. 5327. (Aug. 8, 1997), pp. 809-811.
Stable URL:
http://links.jstor.org/sici?sici=0036-8075%2819970808%293%3A277%3A5327%3C809%3AMACPRP%3E2.0.CO%3B2-0

[6] **A Unified Polymerase Mechanism for Nonhomologous DNA and RNA Polymerase**
T. A. Steitz; S. J. Smerdon; J. Jäger; C. M. Joyce
Science, New Series, Vol. 266, No. 5193. (Dec. 23, 1994), pp. 2022-2025.
Stable URL:
http://links.jstor.org/sici?sici=0036-8075%2819941223%293%3A266%3A5193%3C2022%3AAUPMFN%3E2.0.CO%3B2-U

LINKED CITATIONS

[9] **Interactions of the RNA Polymerase of Bacteriophage T7 with Its Promoter during Binding and Initiation of Transcription**

Richard A. Ikeda; Charles C. Richardson

Proceedings of the National Academy of Sciences of the United States of America, Vol. 83, No. 11. (Jun. 1, 1986), pp. 3614-3618.

Stable URL:

http://links.jstor.org/sici?sici=0027-8424%2819860601%2983%3A11%3C3614%3AIOTRPO%3E2.0.CO%3B2-M

[15] **Crystal Structure at 3.5 \angst Resolution of HIV-1 Reverse Transcriptase Complexed with an Inhibitor**

L. A. Kohlstaedt; J. Wang; J. M. Friedman; P. A. Rice; T. A. Steitz

Science, New Series, Vol. 256, No. 5065. (Jun. 26, 1992), pp. 1783-1790.

Stable URL:

http://links.jstor.org/sici?sici=0036-8075%2819920626%293%3A256%3A5065%3C1783%3ACSA3RO%3E2.0.CO%3B2-W

[18] **Conferring RNA Polymerase Activity to a DNA Polymerase: A Single Residue in Reverse Transcriptase Controls Substrate Selection**

Guangxia Gao; Marianna Orlova; Millie M. Georgiadis; Wayne A. Hendrickson; Stephen P. Goff

Proceedings of the National Academy of Sciences of the United States of America, Vol. 94, No. 2. (Jan. 21, 1997), pp. 407-411.

Stable URL:

http://links.jstor.org/sici?sici=0027-8424%2819970121%2994%3A2%3C407%3ACRPATA%3E2.0.CO%3B2-L

[23] **Structure of a Covalently Trapped Catalytic Complex of HIV-1 Reverse Transcriptase: Implications for Drug Resistance**

Huifang Huang; Rajiv Chopra; Gregory L. Verdine; Stephen C. Harrison

Science, New Series, Vol. 282, No. 5394. (Nov. 27, 1998), pp. 1669-1675.

Stable URL:

http://links.jstor.org/sici?sici=0036-8075%2819981127%293%3A282%3A5394%3C1669%3ASOACTC%3E2.0.CO%3B2-H